Effect of Interpass Temperature in the Single-Layer ER5356 WAAM-GMAW Milling Process on Tool Wear and Surface Roughness

Faza Khoirina[1], Afrizal Riyantono[1], Agus Sifa [1], Agus Sentana[1], Ario Sunar Baskoro [1], Gandjar Kiswanto[1]

[1] Universitas Indonesia, Department of Mechanical Engineering, Faculty of Engineering, Universitas Indonesia, Kampus UI Depok, Depok 16424, Indonesia
ario@eng.ui.ac.id

Abstract. The application of additive manufacturing (AM) techniques is crucial to developing the industrial sector. This method is demonstrated by the use of wire-based methods to achieve effective and efficient production results. Wire arc additive manufacturing (WAAM) is a type of additive manufacturing process that relies on melting metal through an electric arc, allowing metal wires to be arranged to form the desired component gradually. The WAAM process generates residual heat, which must be considered in subsequent post-processing stages, particularly when using milling process. In this study, the WAAM process employed the gas metal arc welding (GMAW) method, using an AA6061 aluminum series substrate and ER5356 filler material. The research applied the Johnson-Cook method and conducted experiments at interpass temperatures of 100°C, 150°C, and 200°C to investigate the effects of the WAAM-GMAW process on tool wear and surface roughness at specific interpass temperatures during milling process. The methodology involved milling process modeling with a cutting depth of 0.3 mm, as well as experiments to measure cutting stress, tool wear, and surface roughness quality. The results showed a change in tool diameter after the milling process, from 10.654 mm to 9.824 mm. At a weld bead temperature of 200°C, the shortest cooling time was observed, which contributed to minimizing tool wear. However, the surface roughness of the weld bead was high, measured at 1.732 µm. This result was caused by the elevated temperature of the weld bead, which reduced hardness, induced oxidation and diffusion, resulting in unstable cutting and increased surface roughness.

Keywords: ER5356, GMAW-Milling, Hybrid-WAAM, Roughness, Tool Wear

1 Introduction

In various industries, wire arc additive manufacturing (WAAM) is crucial due to its impact on progress, cost, and environment [1]. WAAM is a type of 3D printing in which metal components are created layer by layer by melting metal wire using an electric arc. WAAM, using metal inert gas (MIG) welding or gas metal arc welding (GMAW),

S. C. Asih et al. (eds.), *Proceedings of the 19th International Conference on Quality in Research (QiR 2025)*, Advances in Engineering Research 303,
https://doi.org/10.2991/978-94-6239-717-0_15

can deposit material at rate of 3-4 kg per hour [2][3] . The benefits of WAAM-GMAW include rapid material deposition, the ability to produce large-sized components, lower costs, increased efficiency, and the opportunity to repair defective components [1]. While high deposition rates accelerate production and improve quality, efficiency, and performance, they also pose challenges in the manufacturing process [4]. Heat accumulation during the GMAW process causes grain growth and a decrease in the mechanical properties of the deposit [5]. Cooling during the WAAM process is crucial to address heat buildup at the joint temperature, aiming to reduce heat input, residual stresses, and distortion in fabricated components [6]. Hybrid WAAM is revolutionizing modern metal manufacturing, improving productivity and component quality [7]. The benefits of heat buildup reduction come from the use of GMAW equipment, such as milling, after the WAAM process [8]. Factors affecting the efficiency of the hybrid process include thermal effects within the material and residual stresses [9]. Imperfect parameters such as current and voltage fluctuations, as well as unstable speed control, lead to irregular surface geometries in WAAM. The solution is to improve surface precision by incorporating milling processes after the welding stage, which can lead to optimization of the resulting product.

Several studies on the WAAM-GMAW process have been conducted using aluminum-based materials. Jose L. used aluminum materials, specifically ER5356 and AA6063-T5, applying the Taguchi method in the GMAW process [10]. The GMAW process used AA5356 filler metal and AA5038 base material. They observed the structure and strength of the AA5356 welds [11]. The study investigated bead formation when using ER4043 aluminum wire on an Al6061-T6 base, by varying the welding current during GMAW [12]. In another study, filler materials ER5356 and ER1100 were used in conjunction with the GTAW process, based on WAAM, to investigate the effects of polarity and current strength on multilayer deposition [13]. Other studies have shown that air cooling can improve mechanical properties and stabilize the deposition process [14]. Some approaches involve natural cooling of the component or substrate during deposition [15]. Air cooling techniques have been proven effective and efficient [16]. Cooling strategies include dwell time cooling and interlayer air cooling during the WAAM process [17].

Benquan Li performed robotic-based WAAM-Milling on AA5356 material and found that the surface quality of the milled parts improved significantly. However, surface roughness, cutting temperature, cutting force, and porosity caused by WAAM still affected the mechanical properties [18]. According to Nguyen, the Milling process produced the best surface finish, where surface roughness was influenced by spindle speed [19]. Jia modeled the Johnson-Cook behavior of AA6061-T6 material by modifying the strain rate, achieving 45.68% accuracy with strain rates ranging from 0.1 to 100/s [20]. Meanwhile, Li conducted experiments on AA6061-T6 using a CNC machine and a Kistler dynamometer, comparing simulated and experimental cutting forces, resulting in a maximum error of +9.97% [21]. T. Mac found that tool wear and surface roughness significantly decreased when Milling SKD11 at a speed of 600 m/min and a temperature of 500°C, by 82.47% (95.74%) and 91.08%, respectively [22]. Furthermore, S. Akram reported, that higher orthogonal cutting speeds reduced cutting forces due to adiabatic heating and shorter contact times between the tool and the workpiece [23].

According to H. Tian using the Response Surface Methodology (RSM), an increase in temperature softened the AA2219 material, reducing both external cutting force and internal stress through finite element simulations, as supported by an R value of 0.8247 [24]. Additionally, the low spindle speed and feed rate during the Milling process initially increased, then significantly reduced surface roughness, consistent with lower temperatures, as shown in experiments [25]. Through FEM simulation using ABAQUS, demonstrated that in 2D orthogonal cutting after the WAAM process, temperature became a significant factor in thermal cutting [9].

Based on the literature review, the Hybrid WAAM-GMAW Milling process requires an effective timeframe post-WAAM fabrication, where milling is directly carried out following the WAAM process using ER5356. This study can improve previous studies by using ER5356 filler, a 5xxx series aluminum alloy with excellent strength, corrosion resistance, and weldability. This study aims to optimize the machining parameters of a 10 mm HSS endmill after GMAW welding, focusing on the influence and management of temperature variations on the weld bead to improve tool life and surface quality [26]. Further research is also needed on the use of ER5356 aluminum filler on AA6061 substrates. This study applies the Johnson-Cook method and interpass temperature experiments on a single layer. This research innovation is focused on analyzing the geometry of tool wear, surface roughness, ER5356 layer temperature, and von Mises stress results through the Johnson-Cook method, following the post-process milling stage.

2 Materials and Methods

2.1 Materials

The aluminum alloy plate material, with the AA6061 series, used in the Hybrid WAAM-GMAW Milling process experiment, served as the substrate, having dimensions of 150 mm × 50 mm × 6 mm. The filler material used was ER5356 wire with a diameter of 1.2 mm, and its compositional specifications are shown in Table 1.

Table 1. Composition of AA6061 and Filler ER5356

Material	Al	Si	Fe	Cu	Mn	Mg	Zn	Ti
Substrate AA6061 [18]	Bal	0.25	0.40	0.10	0.05-0.20	5.0	0.1	-
Filler ER5356 [27]	Bal	0.40-0.80	0.33	0.15-0.40	Max 0.15	0.81-1.20	Max 0.25	Max 0.15

The surface of the AA6061 substrate was ground and then polished using an acetone cleaner before testing. This process was followed by the GMAW welding process using ER5356 filler metal. Table 2 and 3 present the parameters used in the Hybrid WAAM GMAW-Milling process.

Table 2. WAAM-GMAW parameter settings

Parameter	Range
Welding Current	170 A
Voltage	13.3 V
Gas flow rate	25 l/min
CTWD	20 mm
Travel Speed	110 mm/min
Feed rate	140 mm/s

Table 3. Milling parameter settings

Parameter	Range
Feed rate Milling	80 mm/s
Spindle Speed Milling	4500 rpm

2.2 Methods

In this research, several process stages will be carried out. The stages of the research process that will be analyzed are shown in Fig. 1. Starting with a literature review, preparing tools and materials, identifying parameters to obtain optimal welding results. This process will be continued with Hybrid WAAM GMAW experiments with interpass temperatures determined at 100°C, 150°C, and 200°C. After that, if the condition of the weld bead size is in accordance with AWS standards, the Milling process can be continued. If not, it is repeated at the welding parameter identification stage. After the Milling parameter identification is found, experiments are continued with a cutting depth of 0.3 mm at each interpass temperature parameter. This research will then continue with surface roughness testing, tool wear conditions, and simulation comparisons.

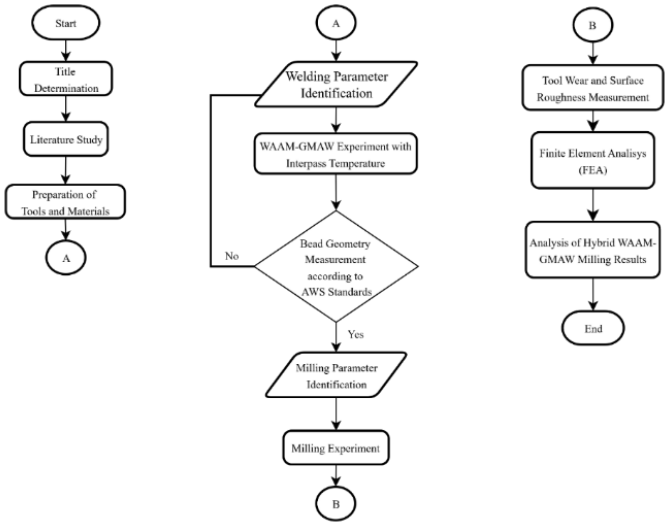

Fig.1. Flow diagram

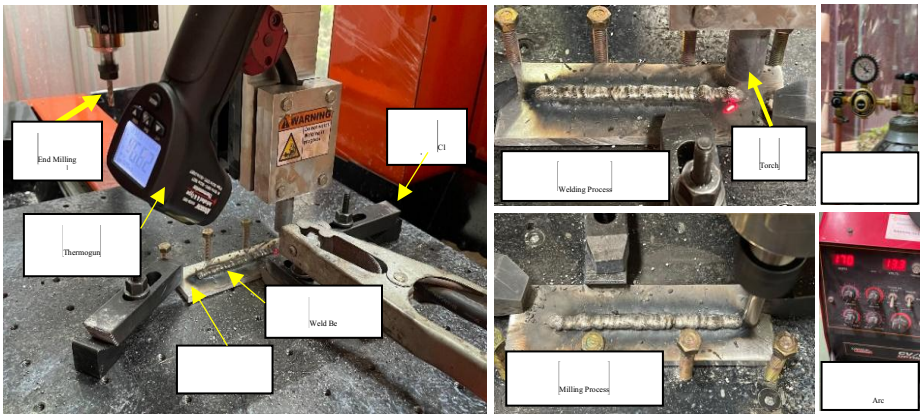

Fig. 2. Set-up hybrid WAAM-GMAW milling machine

The Hybrid WAAM process uses the Gas Metal Arc Welding (GMAW) method followed by a milling process, as shown in Fig. 2. The main elements of this experimental setup consist of a GMAW welding machine, a welding and milling chamber, argon shielding gas, a thermogun, and a wire feeder. The GMAW welding machine and welding chamber serve as the GMAW welding process sites. The milling chamber is used to perform the milling process. The argon shielding gas protects the molten weld metal from atmospheric contamination, which can cause weld defects. The thermogun measures the accumulated temperature during the WAAM GMAW process, and the wire feeder supplies the welding wire.

The Hybrid WAAM GMAW machine used is a Lincoln Electric CV/CC500 Optimarc MIG machine with a router milling machine. Post-processing is performed after the WAAM GMAW process is complete. To achieve precise results after the WAAM process, milling is necessary to smooth out uneven weld surfaces caused by WAAM GMAW (surface waviness).

In this case the machine can be used in industry, because the machines used allow for the process. Can be applied to multi-layer WAAM by implementing interpass temperature control using a cooling system to improve production efficiency. The material behavior during this process can be analyzed using the Johnson-Cook method. To model the Johnson-Cook parameter calculations for ER5356 material, the following Equation 1 can be used [20]:

$$\sigma = (A + B \cdot \epsilon^n)\left(1 + C \cdot \ln\left(\frac{\dot{\epsilon}}{\dot{\epsilon_0}}\right)\right)(1 - T^*)^m \quad (1)$$

In this study, the flow stress (σ) is determined as a function of several variabel, including the equivalent plastic strain (ϵ), strain rate $(\dot{\epsilon})$, and temperature (T). The material behavior is described using empirical constants A, B, C, n, and m which are specific to the material being studied. The reference strain rate $(\dot{\epsilon}_0)$ is typically taken as $10s^{-1}$. To take thermal effects into account, the reduced temperature (T^*) Equation 2 is used, and it is defined as:

$$T^* = \frac{T - T_m}{T_0 - T_m} \quad (2)$$

where T is the current temperature, T_m is the material's melting temperature, and T_0 is the reference temperature, usually corresponding to room temperature. This dimensionless temperature parameter allows the model to incorporate the influence of thermal softening during plastic deformation. The values for ER5356 are assumed based on an approximate reference to the mechanical properties of similar materials, as shown in Table 4.

Table 4. Johnson-Cook parameter of ER5356

Parameter	ER5356
A	150 MPa
B	300 MPa
n	0.45
C	0.015
m	1
T_m	873K
T_0	293K
$\dot{\epsilon}$	0.72 s
$\dot{\epsilon_0}$	$10s^{-1}$

Optimization is performed on the parameters related to tool wear. The heat condition of the weld bead causes rapid degradation of the 10 mm diameter High-Speed Steel (HSS) endmill, which is manifested in the loss of tool hardness and triggers wear mechanisms such as oxidation and diffusion. This condition leads to unstable cutting performance and results in increased surface roughness [28][29].

3 Results and Discussion

3.1 WAAM Experiments

As shown in Fig. 3. Fig. 3a, 3b, and 3c, the results of Hybrid WAAM GMAW Milling welding experiments are presented, with different cooling times according to the respective layer temperatures of 100°C, 150°C, and 200°C. Fig. 4a and 4b shows that the temperature condition of 100°C has the longest cooling time reaching 291 seconds, the temperature of 150°C has a cooling time of 60 seconds and the temperature of 200°C has the fastest time up to 51 seconds. The single-layer condition was chosen to investigate heat dissipation and cooling behavior at the interface between the deposited bead and the substrate.

(a) (b) (c)

Fig. 3. Results of hybrid WAAM-GMAW Milling welding experiments: (a) temperature 100°C, (b) temperature 150°C, and (c) temperature 200°C

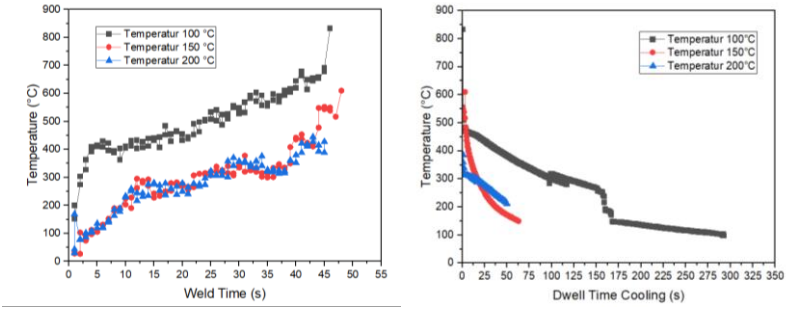

(a) (b)

Fig. 4. Diagram (a) heat accumulation during the WAAM process (b) interpass temperature after natural cooling

Based on the research conducted using the Hybrid WAAM GMAW Milling method with AA6061 aluminum alloy and ER5356 filler, weld bead temperatures of 100°C, 150°C, and 200°C were applied. This study used a heat model or interpass temperature for the direct-Milling filler ER5356, which we used as a reference [25]. The experimental results at different temperatures produced varying dwell times, with shorter dwell times observed at higher temperatures. This result differs from the findings of T. Mac, who reported that tool wear and surface roughness decreased when milling SKD11 at 600 m/min and a temperature of 500°C, by 82.47% (95.74%) and 91.08% [22], respectively. The application of dwell time cooling to achieve precise final results for each component is crucial for industries that require high-quality surfaces, such as aerospace and medical device manufacturing.

3.2 Finite Element Analysis

The data used for the Finite Element Analysis (FEA) simulation also uses the same parameters as those used during the WAAM-GMAW Hybrid Milling experiment process. The temperature, spindle speed, and depth of cut parameters are presented in Table 5. The FEA simulation carried out using Abaqus applies the Johnson-Cook method to determine the strain and stress produced at each different temperature interpass as in Fig. 5 and Fig. 6 shows the results of the strain and stress von mises values based on

the simulation results carried out at temperature interpasses, namely a temperature of 100°C with a strain of 3.089% and a stress of 22.29 MPa, a temperature of 150°C with a strain of 3.103% and a stress of 18 MPa and at a temperature of 200°C with a strain of 3.148% and a stress of 15.82 MPa. FEA allows analysis during the deposition process when the weld bead is in a single-layer state, thus providing a basis for optimizing the interpass temperature deposition strategy.

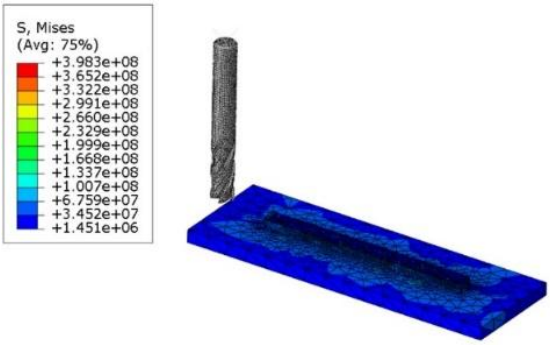

Fig. 5. WAAM GMAW Milling Single Layer

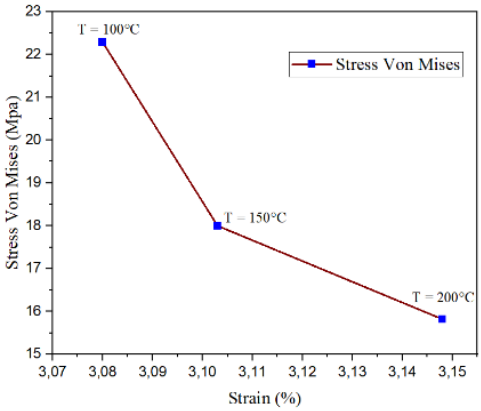

Fig. 6. Strain and Von Mises Stress curve

The comparison of Von Mises Stress results from the experiment and the simulation using the Johnson-Cook model is presented in Table 5 and Fig. 7. The Johnson-Cook method is used to calculate the Von Mises stress value in the WAAM GMAW experiment using the following calculation by Equations 1 and 2.

Table 5. Comparison of simulation and experimental Stress Von Mises

No	Temperature °C	Stress		Strain %
		Simulation	Experiment	
		MPa	MPa	
1	100	22.29	34.04	3.089
2	150	18	55.27	3.103
3	200	15.82	76.51	3.148

At the temperature interpass value of 100°C the simulation stress results show a value of 22.29 MPa, the temperature interpass 150°C shows a simulation stress result of 18 MPa and for the temperature interpass 200°C the simulation stress result is 15.82 MPa. Meanwhile, for the experimental stress results at the temperature interpass 100°C the stress result is 34.04 MPa, at the temperature interpass 150°C the stress result is 55.27 MPa and at the temperature interpass 200°C the stress result is 76.51 MPa. A normalized scale can help interpret the relative differences between simulated and experimental trends compared to a linear interval numeric scale. Using a normalized scale for stress values helps clarify the comparison between simulated and experimental trends. So it can be seen in Fig. 7 that the simulation stress results graph decreases, and the experimental stress results graph increases.

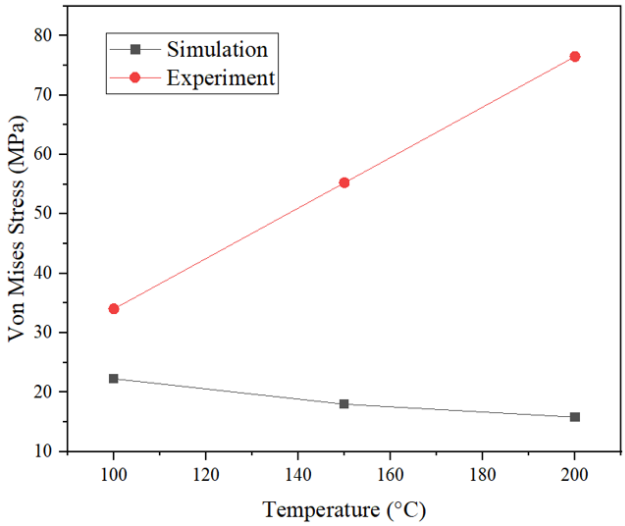

Fig. 7. Comparison of simulation and experimental stress yield curves

Simulation results are usually higher or lower than experimental results. This occurs because simulations use perfect conditions and simple, uniform settings. In real experiments, small errors occur, and not everything is perfectly modelled. These differences depend on the complexity of the material, the type of material, and the accuracy of the measurements during the experiment. Since Johnson–Cook parameters specifically for ER5356 are scarcely reported in the literature, this study employed parameters from aluminum alloys with comparable compositions. This approach is considered reasonable to represent the general thermo-mechanical behaviour and to capture comparative trends. Nevertheless, differences in strain hardening and thermal softening among alloys may lead to deviations from the actual material response, which is acknowledged as a limitation of this study. This study did not include a sensitivity analysis to evaluate the influence of parameter uncertainties on the simulation outcomes. Conducting such an analysis was not feasible and is acknowledged as a limitation of this work. Further research is therefore recommended.

3.3 Milling Experiment

3.3.1 Tool Wear

The 10 mm HSS endmill, with 4 flutes, used during the experiment, exhibited geometric changes due to flank wear. As shown in Fig. 8, the initial diameter of the HSS endmill, measured using a Dino-lite, was 10.65 mm, which decreased to 9.82 mm. Higher weld bead layer temperatures resulted in lower tool wear values, as illustrated in Fig. 9. At high spindle speeds, cutting forces and temperatures can be reduced due to the thermal softening effect [21]. The measurement data is displayed with error bar charts to help validate data consistency and demonstrate significant differences in results.

(a) (b)

Fig. 8. Condition tool wear (a) before and (b) after

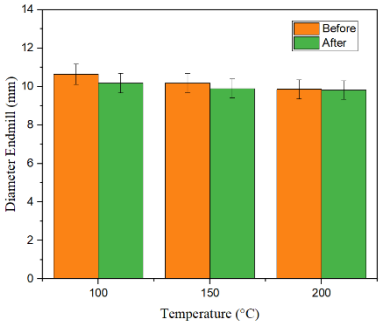

Fig. 8. Diameter of tool wear endmill HSS 10 mm

Based on the experiment, have a limit of the topic discussion to knowing tool wear. This research differs from other studies that address microstructure and hardness. Lower tool wear was observed when milling was performed on the weld bead in a hot condition. This situation is uncommon in Milling processes, as several other studies have stated that performing Milling on a still-hot weld bead significantly increases both tool wear and surface roughness [30]. In contrast, this study observed low tool wear at high weld bead temperatures. This includes the softened state of the weld material, which significantly reduces cutting forces due to its high thermal conductivity, the relaxation of residual stresses due to repeated thermal cycling, and the formation of a

protective oxide layer that reduces friction. In this case, just an analysis of the flank wear section was observed.

3.3.2 Surface Roughness

Surface roughness was measured using the SURFCOM 2900SD3-12 device, as shown in Fig. 10, to determine the surface roughness values resulting from the Hybrid WAAM GMAW Milling process. The measurements followed ISO 21920 standards, which provide values for Ra, Rq, and Rz. Measurements were taken over a 5 mm length. The surface roughness measurement results are presented in Fig. 11, and the corresponding Milling tool mark pattern is shown in Fig. 12. Visually and based on measurements, the surface appeared rougher at a temperature of 200°C before Milling compared to the 100°C condition.

Fig. 9. Surface roughness measurement tool

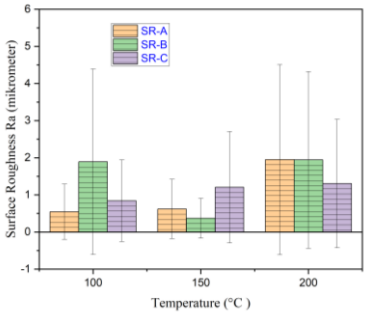

Fig. 10. ER5356 filler surface roughness results

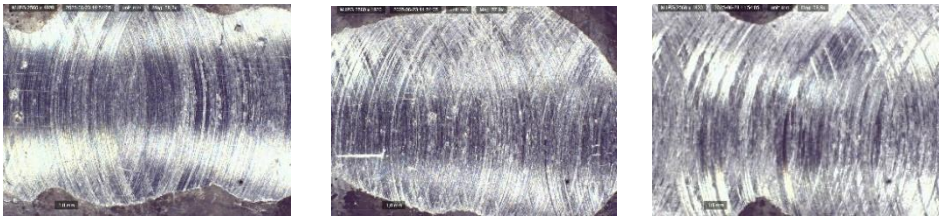

(a) Temperature 100°C (b) Temperature 150°C (c) Temperature 200°C

Fig. 12. Surface Roughness After Milling

High weld bead temperatures can affect surface roughness and tool wear conditions, resulting in lower strain and von Mises stress values. Surface roughness values tend to be higher at elevated temperatures. This result is due to increased heat input, which may lead to uncontrolled melting or spatter formation, thereby increasing surface roughness consistent [31]. A hot weld bead causes the tool to lose its hardness, leading to oxidation and diffusion, which results in unstable cutting and higher surface roughness [28].
Table 6 shows that this experiment used a spindle speed of 4500 rpm and a cutting depth of 0.3 mm. This resulted in different changes in the geometry of the endmill at each temperature interpass, with surface roughness values increasing with increasing temperature. Furthermore, longer cooling times were required at lower temperature interpass values.

Table 6. Experimental parameters and outcomes of hybrid WAAM GMAW milling

No.	Temperature (°C)	Spindle speed (rpm)	Depth of cut (mm)	Tool geometry D (mm)		Measurement difference D (mm)	Roughness (μm)			Dwell time (s)
				Before	After		A	B	C	
1	100	4500	0.3	10.65	10.19	0.23	0.5454	1.8904	0.842	291 s
2	150	4500	0.3	10.19	9.90	0.15	0.6209	0.3709	1.2053	60 s
3	200	4500	0.3	9.86	9.82	0.02	1.9505	1.9409	1.3046	51 s

This study employed a welding process that combined the Hybrid WAAM GMAW Milling method with AA6061 aluminum alloy and ER5356 filler. The analysis results can be concluded as follows: The temperature parameters for the Milling process used after the GMAW process were divided into three levels: 100°C, 150°C, and 200°C, with the fastest dwell time cooling occurring at the highest temperature condition. The strain values from the GMAW Milling simulation at weld bead temperatures of 100°C, 150°C, and 200°C were 3.089%, 3.103%, and 3.148%, respectively. The corresponding von Mises stress values were 22.29 MPa, 18 MPa, and 15.82 MPa. The Finite Element Analysis (FEA) results performed on GMAW Milling weld bead measurements significantly contributed to the distribution of the maximum Von Mises stress, which is used to indicate the transition between the weld metal and the HAZ. FEA allows analysis during the deposition process when the weld bead is in a single-layer state, thus providing a basis for optimizing the interpass temperature deposition strategy. Tool wear and surface roughness values depend on the temperature of the ER5356 weld bead before the milling process. At a temperature of 100°C with a cooling time after welding of 291 s, a smoother surface is produced. Milling at a spindle speed of 4500 rpm on weld beads with different temperatures resulted in high tool wear at 100°C, but low tool wear at 200°C. This result is due to the hot and softened condition of the weld bead material, which significantly reduces cutting forces and allows rapid heat dissipation due to its high thermal conductivity. In this study, only one test was carried out at each interpass

temperature conditions. Surface roughness at a weld bead temperature of 200°C was higher than at 100°C. This result is influenced by the hot condition of the weld bead, which causes the tool to lose hardness, leading to oxidation and diffusion, resulting in unstable cutting and increased surface roughness. The Johnson-Cook parameters of ER5356 used in this study affected the resulting strain and von Mises stress values.

Acknowledgements
This research is supported by the PUTI Q2-Year 2024 from the University of Indonesia, contract number: No. NKB-698/UN2.RST/HKP.05.00/2024.
The authors would like to thank the National Research and Innovation Agency (BRIN) for providing the facilities necessary to successful implementation of the simulation test using Abaqus. This support significantly contributed to the smooth running of the research.

References

[1] W. Hackenhaar, J. A. E. Mazzaferro, F. Montevecchi, and G. Campatelli, "An experimental-numerical study of active cooling in wire arc additive manufacturing," *J. Manuf. Process.*, vol. 52, no. January, pp. 58–65, 2020, doi: 10.1016/j.jmapro.2020.01.051.

[2] K. E. K. Vimal, M. Naveen Srinivas, and S. Rajak, "Wire arc additive manufacturing of aluminium alloys: A review," *Mater. Today Proc.*, vol. 41, pp. 1139–1145, 2019, doi: 10.1016/j.matpr.2020.09.153.

[3] Z. Wang and Y. Zhang, "A review of aluminum alloy fabricated by different processes of wire arc additive manufacturing," *Medziagotyra*, vol. 27, no. 1, pp. 18–26, 2021, doi: 10.5755/j02.ms.22772.

[4] N. A. Rosli, M. R. Alkahari, M. F. bin Abdollah, S. Maidin, F. R. Ramli, and S. G. Herawan, "Review on effect of heat input for wire arc additive manufacturing process," *J. Mater. Res. Technol.*, vol. 11, no. February, pp. 2127–2145, 2021, doi: 10.1016/j.jmrt.2021.02.002.

[5] A. K. Sinha, S. Pramanik, and K. P. Yagati, "WAAM of Al–Cu Alloy: Effect of Cooling and Remelting on Grain Size and Mechanical Properties," *Trans. Indian Inst. Met.*, vol. 76, no. 5, pp. 1331–1339, 2023, doi: 10.1007/s12666-022-02857-2.

[6] I. Mishra and R. Srivastava, "Thermal simulation of Al alloy developed by wire arc additive manufacturing using finite element analysis," *Int. J. Interact. Des. Manuf.*, pp. 6875–6883, 2024, doi: 10.1007/s12008-024-01973-1.

[7] R. Sarma, S. Kapil, and S. N. Joshi, "Development of a framework for computer aided design and manufacturing of 3 axis hybrid wire arc additive manufacturing," *Mater. Today Proc.*, vol. 62, no. P14, pp. 7625–7634, 2022, doi: 10.1016/j.matpr.2022.05.011.

[8] J. L. Prado-Cerqueira, J. L. Diéguez, and A. M. Camacho, "Preliminary development of a Wire and Arc Additive Manufacturing system (WAAM)," *Procedia Manuf.*, vol. 13, pp. 895–902, 2017, doi:

10.1016/j.promfg.2017.09.154.

[9] H. Tian, Z. Lu, S. Chen, and X. Yu, “Simulation of Thermally Assisted Cutting of the Aluminum Alloy after WAAM,” vol. 165, no. Smont, pp. 83–86, 2019, doi: 10.2991/smont-19.2019.20.

[10] J. L. Meseguer-Valdenebro, E. Martínez-Conesa, and A. Portoles, “Influence of welding parameters on grain size, HAZ and degree of dilution of 6063-T5 alloy: optimization through the Taguchi method of the GMAW process,” *Int. J. Adv. Manuf. Technol.*, vol. 120, no. 9–10, pp. 6515–6529, 2022, doi: 10.1007/s00170-022-09094-3.

[11] A. Muthukumaran, S. Jeyakumar, and K. Jayakumar, “Metallurgical and mechanical properties of marine grade AA5356 using wire arc additive manufacturing,” *Mater. Res. Express*, vol. 11, no. 7, 2024, doi: 10.1088/2053-1591/ad5817.

[12] K. H. Kazmi, A. K. Das, S. K. Sharma, A. Mandal, and A. K. Shukla, “Wire arc additive manufacturing of ER-4043 aluminum alloy: evaluation of bead profile, microstructure, and wear behavior,” *Weld. World*, vol. 67, no. 9, pp. 2187–2200, 2023, doi: 10.1007/s40194-023-01558-8.

[13] A. Sentana, M. F. Firdaus Subki, M. A. Amat, A. S. Baskoro, and G. Kiswanto, “The Effect of Polarity and Current Strength on Multilayer Wire Arc Additive Manufacturing (WAAM) Based Tungsten Inert Gas (TIG) Welding using ER5356 and ER1100 Welding Wire on SS316 Plates,” *Evergreen*, vol. 11, no. 4, pp. 3341–3347, 2024.

[14] Y. Meng, Z. Li, M. Gao, H. Chen, X. Wu, and Q. Yu, “Laser cleaning assisted wire arc additive manufacturing of aluminum alloy thin-wall through synchronous wire-powder deposition,” *Thin-Walled Struct.*, vol. 197, no. December 2023, 2024, doi: 10.1016/j.tws.2024.111622.

[15] F. Ribeiro, T. Fernando, M. Scotti, V. Lemes, and J. Américo, “Combined effect of the interlayer temperature with travel speed on features of thin wall WAAM under two cooling approaches,” *Int. J. Adv. Manuf. Technol.*, pp. 273–289, 2023, doi: 10.1007/s00170-023-11105-w.

[16] J. Zhang, R. Mao, C. Li, J. Lan, X. Yi, and Z. Zhang, “Optimization air-conditioning system and thermal management of data center via fan-wall free cooling technology,” *Appl. Therm. Eng.*, vol. 234, no. July, p. 121245, 2023, doi: 10.1016/j.applthermaleng.2023.121245.

[17] L. Heinrich, T. Feldhausen, K. Saleeby, T. Kurfess, and C. Saldaña, “Build plate conduction cooling for thermal management of wire arc additive manufactured components,” *Int. J. Adv. Manuf. Technol.*, vol. 124, no. 5–6, pp. 1557–1567, 2023, doi: 10.1007/s00170-022-10558-9.

[18] B. Li, K. M. Nagaraja, R. Zhang, A. Malik, H. Lu, and W. Li, “Integrating robotic wire arc additive manufacturing and machining: hybrid WAAM machining,” *Int. J. Adv. Manuf. Technol.*, vol. 129, no. 7–8, pp. 3247–3259, 2023, doi: 10.1007/s00170-023-12517-4.

[19] N.-T. Nguyen, “A Study on Influence of Milling Types and Cutting Conditions on Surface Roughness in Milling of Aluminum Alloy Al6061-T6,” *Univers. J. Mech. Eng.*, vol. 8, no. 4, pp. 183–190, 2020, doi: 10.13189/ujme.2020.080403.

[20] Z. Jia, B. Guan, Y. Zang, Y. Wang, and L. Mu, "Modified Johnson-Cook model of aluminum alloy 6016-T6 sheets at low dynamic strain rates," *Mater. Sci. Eng. A*, vol. 820, no. December 2020, p. 141565, 2021, doi: 10.1016/j.msea.2021.141565.

[21] S. Li, J. Sui, F. Ding, S. Wu, W. Chen, and C. Wang, "Optimization of Milling Aluminum Alloy 6061-T6 using Modified Johnson-Cook Model," *Simul. Model. Pract. Theory*, vol. 111, no. April 2020, p. 102330, 2021, doi: 10.1016/j.simpat.2021.102330.

[22] T. B. Mac, T. T. Luyen, and D. T. Nguyen, "The Impact of High-Speed and Thermal-Assisted Machining on Tool Wear and Surface Roughness during Milling of SKD11 Steel," *Metals (Basel).*, vol. 13, no. 5, 2023, doi: 10.3390/met13050971.

[23] S. Akram, S. H. I. Jaffery, Z. Anwar, M. Khan, and M. A. Khan, "Toward clean manufacturing: an analysis and validation of a modified Johnson–Cook material model for low and high-speed orthogonal machining of low-carbon aluminum alloy (Al 6061-T6)," *Int. J. Adv. Manuf. Technol.*, vol. 129, no. 5–6, pp. 2523–2536, 2023, doi: 10.1007/s00170-023-12367-0.

[24] H. Tian, Z. Lu, and S. Chen, "Predictive Modeling of Thermally Assisted Machining and Simulation Based on RSM after WAAM," *Metals (Basel).*, vol. 12, no. 4, 2022, doi: 10.3390/met12040691.

[25] H. Tian, Z. Lu, F. Li, and S. Chen, "Predictive Modeling of Surface Roughness Based on Response Surface Methodology after WAAM," vol. 181, no. Ice2me, pp. 47–50, 2019, doi: 10.2991/ice2me-19.2019.11.

[26] G. Prasad, G. S. Vijay, and R. C. Kamath, "Evaluation of tool wear and surface roughness in high-speed dry turning of Incoloy 800," *Cogent Eng.*, vol. 11, no. 1, p., 2024, doi: 10.1080/23311916.2024.2376913.

[27] G. Doumenc *et al.*, "Investigation of microstructure, hardness and residual stresses of wire and arc additive manufactured 6061 aluminium alloy," *Materialia*, vol. 25, no. February, p. 101520, 2022, doi: 10.1016/j.mtla.2022.101520.

[28] M. Necpal and M. Vozár, "Thermal Effects of High-Speed Machining : Analysis of Cutting Zone Temperatures , Tool Behavior , and Cutting Forces in C45 Steel Turning at Elevated Speeds," vol. 94, no. 3, pp. 91–94, 2025.

[29] P. A. Mane, P. A. Dhawale, S. Nipanikar, and A. N. Khadtare, "Predictive Modeling of Surface Roughness, Tool Wear, and Cutting Temperature in High-Speed Turning under Sustainable Machining Environments," *SAE Int. J. Mater. Manuf.*, vol. 19, no. 1, pp. 05-19-01–0007, May 2025, doi: 10.4271/05-19-01-0007.

[30] F. Taufik Rohman and H. Abizar, "Analisis Keausan Pahat Endmill Hss Flute 4 Pada Proses Milling Handle Sepeda Motor," *Kurvatek*, vol. 8, no. 2, pp. 181–192, 2023, doi: 10.33579/krvtk.v8i2.4054.

[31] M. Jamshidinia and R. Kovacevic, "The influence of heat accumulation on the surface roughness in powder-bed additive manufacturing," 2015, doi: 10.1088/2051-672X/3/1/014003.